



Distribution of modern dinocysts in surface sediments of southern Brittany (NW France) in relation to environmental parameters: Implications for paleoreconstructions

Clément Lambert, Aurélie Penaud, Clément Poirier, Evelyne Goubert

► To cite this version:

Clément Lambert, Aurélie Penaud, Clément Poirier, Evelyne Goubert. Distribution of modern dinocysts in surface sediments of southern Brittany (NW France) in relation to environmental parameters: Implications for paleoreconstructions. *Review of Palaeobotany and Palynology*, 2022, 297, pp.104578. 10.1016/j.revpalbo.2021.104578 . hal-03472932

HAL Id: hal-03472932

<https://hal.science/hal-03472932>

Submitted on 8 Jan 2024

HAL is a multi-disciplinary open access archive for the deposit and dissemination of scientific research documents, whether they are published or not. The documents may come from teaching and research institutions in France or abroad, or from public or private research centers.

L'archive ouverte pluridisciplinaire **HAL**, est destinée au dépôt et à la diffusion de documents scientifiques de niveau recherche, publiés ou non, émanant des établissements d'enseignement et de recherche français ou étrangers, des laboratoires publics ou privés.



Distributed under a Creative Commons Attribution - NonCommercial 4.0 International License

**Distribution of modern dinocysts in surface sediments of southern
Brittany (NW France) in relation to environmental parameters:
implications for paleoreconstructions**

Clément Lambert^{1*}, Aurélie Penaud², Clément Poirier³, Evelyne Goubert¹

¹ Univ. Vannes (UBS), UMR 6538 Laboratoire Géosciences Océan (LGO), F-56000 Vannes,
France

² Univ. Brest (UBO), CNRS, UMR 6538 Laboratoire Géosciences Océan (LGO), F-29280
Plouzané, France

³ Univ. Normandie, UNICAEN, UNIROUEN, CNRS, M2C, 14000 Caen, France

*Corresponding author: clement.lambert@univ-ubs.fr

13 Abstract

14 Dinoflagellate cyst assemblages from 15 modern surface sediment samples of the Bay of
15 Quiberon (Southern Brittany shelf) have been examined to assess their **potential as** marine
16 bio-indicators for paleoenvironmental reconstructions in a shallow coastal environment. **Some**
17 **discrepancies are** noted in the distribution of dinocyst **taxa in the study area**, and particularly
18 regarding **dinocyst concentration and diversity (26 different taxa identified in total) as well as**
19 **heterotrophic taxa percentages**. We suggest that the **proportion** of heterotrophic **taxa is**, in an
20 embayment of 15m deep in average, mainly attributed to bottom water oxygenation and
21 sediment granulometry, both acting on species-selective degradation after dinocyst deposition.
22 More precisely, higher heterotrophic abundances are found under lower oxic conditions and in
23 fine grain-size sediment samples, leading to caution about their use as productivity **indicators**
24 in coastal environments when these parameters are not fully addressed. **The** comparison of the
25 Bay of Quiberon data with surface sediment samples and top cores from **previously** published
26 data makes it possible to establish a transect of the modern dinocyst distribution from inshore
27 to offshore areas in the northern Bay of Biscay, allowing to identify different ecological
28 groups according to the hydrological and bathymetric contexts: i) an estuarine assemblage
29 strongly dominated by *Lingulodinium machaerophorum*, ii) a proximal coastal assemblage
30 dominated by *L. machaerophorum* and, to a lesser extent, *Spiniferites bentorii*, iii) a neritic
31 assemblage dominated by *L. machaerophorum*, *Spiniferites ramosus* and cysts of
32 *Pentapharsodinium dalei*, and iv) an oceanic group dominated by *Spiniferites mirabilis* and
33 *Operculodinium centrocarpum*.

34 Keywords: dinoflagellate cysts, marine palynology, taphonomic issues, southern Brittany
35 shelf, paleoenvironmental reconstructions

1. Introduction

Dinoflagellates (currently about 2,377 species known; *Gomez, 2012*) are eukaryotic unicellulars found in most aquatic environments, mainly in marine waters and in the upper part of the water column, and play an important role in the trophic network (*Dale, 1996*). Half of them are heterotrophic and feed on other dinoflagellates, microalgae, diatoms and organic debris in the water column (*Evitt, 1985; Dale, 1996*); the other half possesses chloroplasts (*Gomez, 2012*). As the vegetative growth of heterotrophic dinoflagellates is likely to be enhanced by prey availability (e.g. diatoms, autotrophic dinoflagellates, phytodetritus), they are commonly used as : i) productivity tracers in the marine realm (i.e. upwelling areas, e.g. *Radi and de Vernal, 2004; Pennaud et al., 2016; Hardy et al., 2018*) as well as ii) eutrophication tracers in coastal and estuarine areas (e.g. *Dale, 1999; Matsuoka, 1999; Sangiorgi and Donders, 2004; Pospelova and Kim, 2010; Price et al., 2017, 2018; Garcìa-Moreiras et al., 2018*).

Fossilizable organic-walled dinoflagellate cysts (i.e., resting cysts corresponding to “dormant stages” mainly produced during sexual reproduction; e.g., *von Stosch, 1973*) show their highest concentrations in neritic and coastal areas (i.e. where dinoflagellate blooms can occur; *Taylor, 1987*). Organic-walled dinoflagellate cysts (dinocysts) thus represent an important group of microfossils well preserved in sediments. Previous studies carried out on modern marine sediments showed their worldwide distribution as being mainly driven by sea-surface environmental parameters such as temperature (SST for Sea-Surface Temperature), salinity (SSS for Sea-Surface Salinity), sea-ice cover duration in high latitudes, nutrient concentrations and related primary productivity regimes, as well as inshore-offshore gradients, allowing their use as powerful paleoceanographic tracers (e.g., *Dodge and Harland, 1991; Mudie et al., 2001; Marret and Zonneveld, 2003; de Vernal et al., 2013, 2020*;

Zonneveld et al., 2013; Marret et al., 2020; Van Nieuwenhove et al., 2020). However, studies on the current dinocyst diversity, concentration and distribution in coastal environments are scarce, especially for the French coasts. Along the Brittany's coasts, first steps towards understanding of the modern distribution of coastal to oceanic dinocyst taxa were initiated by *Reid (1972), Morzadec-Kerfourn (1977), Wall et al. (1977), Larrazabal et al. (1990)*, recently complemented by *Ganne et al. (2016)* for the Loire estuary and *Lambert et al. (2017)* for the Bay of Brest. A recent spatio-temporal (i.e. in space and time) Holocene study discussed the nearshore-offshore dinocyst distribution on both sides of the freshwater front in the northern Bay of Biscay shelf (*Penaud et al., 2020*). Dinocyst species were then classified in four groups accounting for different hydrological contexts (i.e, estuarine; shallow bay to inner neritic; Iroise Sea or neritic; outer neritic to full oceanic) due to a marine (i.e. distal or offshore) to coastal (i.e. proximal or onshore) transect ranging from 2,174 m to 8 m water depth (*Penaud et al., 2020*).

In this study, we investigated 15 new surface sediment samples collected in the Bay of Quiberon (BQ), which will improve the discussion of the modern spatial dinocyst distribution in a shallow bay environment, especially focusing on rarely addressed taphonomic processes. Then, these data were compared to top cores retrieved in the southern Brittany shelf (*Naughton et al., 2007; Zumaque et al., 2017; Penaud et al., 2020*) and to surface sediments of the Loire estuary mouth (*Ganne et al., 2016*) in order to improve the understanding of the modern spatial dinocyst distribution along a macro-regional inshore-offshore transect.

2. Environmental and geographical settings of the Bay of Quiberon

The ‘Mor Bras’ (Fig. 1) is a bathymetric depression bordering the southern coast of Brittany. It is partially isolated from the general oceanic circulation of the Bay of Biscay and from the high energetic Atlantic swells due to a belt of shoals in the extension of the Quiberon peninsula (Fig. 1). The Bay of Quiberon (BQ), which occupies the western part of the Mor Bras, is a shallow coastal embayment (15 m depth in average) that has been submerged during the Holocene (Baltzer *et al.*, 2014; Menier *et al.*, 2014). A vast network of flooded valleys converges into the Teignouse Strait (TS on Fig. 1) which separates the Quiberon Peninsula from the Houat Island (Vanney, 1965; Menier *et al.*, 2014; Fig. 1). This strait is burrowed by strong tidal currents joining the inlet of the Gulf of Morbihan and contributing to the partial isolation of the BQ from the rest of the Mor Bras by the establishment of tidal gyres (yellow arrows on Fig. 1; Vanney, 1965; Lemoine, 1989; Tessier, 2006).

Recent works carried out in the BQ, following high summer mortality of oysters (Mazurié *et al.*, 2013a, b; Stanisière *et al.*, 2013), have shown that the shallower parts of the BQ (between 0 and 6 m deep) are mainly composed of sandy sediments, due to strong wind-forced water column mixing, while the deepest parts of the BQ are covered with muddy sediments. This sediment distribution is associated with a heterogeneous distribution of benthic foraminiferal species, analyzed in the framework of the RISCO project (‘Comité régional de la conchyliculture Bretagne Sud’ and Ifremer; 2010-2013; coord. J. Mazurié; Mazurié *et al.*, 2013a, b; Stanisière *et al.*, 2013). Among the high foraminiferal diversity studied, some taxa are characteristic of the deepest and fine grain-sized BQ areas (i.e. *Criboelphidium gerthi*, *Elphidium earlandi*, *Gavelinopsis nitida*, *Lagena sulcata*, *Lagena semistriata*, *Lamarckina haliotide*, *Planorbulina mediterraneensis*, *Trifarina angulosa*, and *Textularia truncata*). They form the ‘deepest foraminiferal assemblage’, noted ‘DeepForam’ hereafter.

3. Methods

3.1. Sampling and environmental parameters

3.1.1. Data collection

The sampling campaign was carried out in 2010 in the framework of the RISCO project in 15 sites within the BQ using a 50 x 50 cm Van Veen grab for the optimal preservation of surface sediments (Mazurié *et al.*, 2013a, b; Stanisère *et al.*, 2013; Fig. 1). The first cm of each site was sampled (Table 1) for grain-size and microfossil analyses. All samples were stored in sealed vials with ethanol.

For grain-size analyses, sediments were passed through a column of sieves with different sizes of apertures (i.e. 2 mm, 500 µm, 125 µm and 45 µm). Averaged percentages of the fine sediment fraction (i.e. <125 µm, referred to as ‘granulo<125’ hereafter; Table 2) were considered in this study (Mazurié *et al.*, 2013a, b; Stanisère *et al.*, 2013).

In addition, we compiled the monthly measurements of the bottom water physico-chemical parameters measured at each station to obtain averaged values for the year 2010 (Table 2). Bottom water temperature (referred to as ‘Temp’ hereafter), bottom water salinity (‘Sal’), dissolved oxygen concentration in bottom waters (‘O2’), bottom water turbidity (‘Turb’) and Chlorophyll a concentration in bottom water (‘Chla’) were measured with an MP6 probe (NKE). In addition, bottom water samples were taken from each station to calculate the suspended matter concentration (‘SM’) using vacuum pump filtration. Annual averaged values will be considered in this study (Table 2).

3.1.2. Correlation matrix of variables

A correlation matrix of variables was performed with the “Analysis Toolpack” of Microsoft Excel 2016, to assess the relationship between: i) sedimentological (‘granulo<125’, subsection 3.1.1) and foraminiferal (‘DeepForam’, section 2) data, ii) dinocyst data (‘Cdino’, subsection 3.2.1.; and ‘Srdino’, ‘Hdino’, subsection 3.2.2.) and iii) the measured environmental variables (‘Depth’, ‘Temp’, ‘Sal’, ‘O2’, ‘Chla’, ‘Turb’, ‘SM’, subsection 3.1.1).

The matrix consists of Pearson correlation coefficients (r) between each variable that range from -1 to 1. If r=0, no linear correlation exists between compared variables. The greater the absolute value of r, the stronger the correlation: positive when approaching 1 and negative when approaching -1. Statistical significance is expressed by the p-value. P-value < 0.05 indicates a strong presumption against the null hypothesis and a good confidence in the statistical correlation expressed by the Pearson coefficients.

3.2. Dinoflagellate cyst analysis

3.2.1. Laboratory procedure for palynological slides

Dinocyst extraction was performed at the UMR 6538 CNRS (LGO-*Laboratoire Géosciences Océan*, UBO-University of Brest) from the 10–150 µm sediment fraction. Three cm³ of fifteen BQ surface sediment samples (samples from December 2010) were analyzed following a standard protocol described by *de Vernal et al. (1999)* that includes 10% cold HCl and 70% cold HF to remove carbonate and siliceous fractions, respectively. The final residues were mounted between slides and coverslips with glycerol. Dinocyst concentrations (‘Cdino’; Table 2), expressed in number of cysts per cm³ of dry sediments (cysts/cm³) were calculated thanks to the marker grain method (*Stockmarr, 1971; de Vernal et al., 1999; Mertens et al., 2009*). This method consists in adding aliquot volumes of *Lycopodium* spores before the

palynological treatment, these exotic spores being counted in parallel with fossilized palynomorphs.

3.2.2 Dinocyst identification, diversity indexes and statistical analysis

For each analyzed sample, except BQ sample n°3 (cf. Fig. 1), a minimum of 150 dinocysts was reached, using an Olympus CH-2 optical microscope (at magnifications $\times 630$ and $\times 1000$), in order to provide robust assemblages from a statistical point of view. The threshold of 100 individuals is indeed required to identify 99% of major ($>5\%$) species (*Fatela and Taborda, 2002*) and thus robust to discuss the proportion of the two large groups of dinocysts (i.e. the strict heterotrophic taxa vs. the other dinocysts). The BQ sample n°3, mainly characterized by coarse sediments (i.e. 63% of grain sizes exceed $125\mu\text{m}$), must be interpreted with caution since only 13 specimens were counted. Taxa identification followed *Rochon et al. (1999)*, *Zonneveld & Pospelova (2015)* and *Van Nieuwenhove et al. (2020)*. Dinocyst percentages were calculated for each taxon (list of identified taxa in Table 3), on a main sum including all taxa and excluding non-identified ones (always less than three undetermined specimens per analyzed level).

We use the Shannon Diversity index to estimate the dinocyst diversity as an additional ecological indicator (noted 'Srdino' hereafter for Species Richness; Table 2). The Shannon index provides information both on specific richness and on the structure of populations. The higher the value, the greater the taxa diversity and the more homogeneous the relative abundances. In addition, we calculated the total percentages of brown cysts from heterotrophic dinoflagellates, or heterotrophic dinocysts ('Hdino'; Table 2). Cluster analysis was also conducted on the 15 samples, using PAST v.1.75b (*Hammer et al., 2001*), according

to dinocyst assemblages to better highlight similarities and differences between analyzed samples.

3.2.3 Inshore-offshore transect

In order to discuss dinocyst diversity changes along an inshore-offshore gradient on a larger-scale, we also compared dinocyst assemblages from surface sediments and core tops taken in the northern Bay of Biscay, in different environmental and bathymetric contexts: i) two samples taken in the downstream Loire Estuary (*Ganne et al., 2016*) are representative of the Loire river mouth, ii) the averaged 15 surface samples of this study account for the shallow coastal BQ, iii) a sample from the top core section (level 47 cm) of the CBT-CS11 core (73 m water depth) is representative of the shelf under mixed oceanic and winter fluvial influences (*Penaud et al., 2020*), iv) a sample from top core section (level 4 cm) of the VK03-58bis core (97 m water depth) is representative of the deeper shelf (*Naughton et al., 2007*). Regarding these last two sites, we targeted the two “modern” samples on the basis of palynological evidence unambiguously **signaling** for their contemporaneity (i.e., presence of pollen grains of *Zea mays*). The distal MD95-2002 core, taken off the Armorican margin at 2,200 m deep, has finally been added to the transect (*Zumaque et al., 2017*). The top core sample (0 cm) is estimated at ca. 1,000 Cal. years BP and is therefore representative of late Holocene conditions (*Zumaque et al., 2017*). Such a gradient in dinocyst distribution as a function of the distance to the coast therefore provides a baseline reference for inferring dinocyst-derived past environmental changes on the temperate north-eastern Atlantic margin.

4. Results

4.1. Cluster analysis between study samples

All studied stations are represented within the BQ with a colour code corresponding to the result of the cluster analysis (Figs. 2a, b).

Station n°3 stands out from the others with a low similarity coefficient (i.e. around 0.65; Fig. 2a). The coarse grain size (Fig. 2h) and the related very low dinocyst concentration (Figs. 2c and 3a) characterizing this station set it apart from the others. With the exception of station n°5, all stations located below the 6 m isobath (n°2, 10, 15, 11, 13, 12, 8, and 14) are grouped together in a same cluster (brown colour, Figs. 2a,b) with a high coefficient of similarity (> 0.825; Fig. 2a), and stations located above the 6 m bathymetric threshold (n°4, 6, and 9) are grouped in a same cluster (green colour, Figs. 2a,b) with the additional sites n°7 and 1. All these shallowest sites are characterized by generally coarser grain-size values (Fig. 2h).

4.2. Dinoflagellate cyst results

Dinocyst concentrations of the 15 surface sediment samples range from ca. 300 to 18,300 cysts/cm³ with a mean of ca. 8,100 cysts/cm³ (standard deviation of ca. 5,300 cysts/cm³) (Fig. 3a). The lowest values correspond to the shallowest sites located to the north and west of the BQ whereas the highest ones are recorded at the deepest sites, below the 6 m isobath (Figs. 2c and 3a).

A total of 26 different dinocyst taxa was identified (12 autotrophic and 14 heterotrophic taxa; cf. Table 3) with an average of 14 different taxa per sample (Fig. 3a). Assemblages (Figs. 3a,b) are largely dominated by *Lingulodinium machaerophorum* (45 % in average; Fig. 3b), commonly found dominant in areas with strong fluvial influences (Morzadec-Kerfourne,

1977; Ganne et al., 2016; Lambert et al., 2017; Penaud et al., 2020). The other major autotrophic taxa are *Spiniferites bentorii* (11 % in average; Fig. 3b), *Spiniferites membranaceus* (6 % in average; Fig. 3b) and cysts of *Pentapharsodinium dalei* (5 % in average; Fig. 3b).

The heterotrophic rate is on average 20 % over the whole BQ (Fig. 3b) and is particularly represented by *Brigantedinium* spp. species (i.e. “round brown” cysts produced by *Protoperidinium* dinoflagellate species) (12 % in average; Fig. 3b). The highest relative abundances of heterotrophic cysts (Figs. 2e, 3a) are generally observed in the deepest areas of the BQ (Fig. 2), between 6 and 10 m, which are characterized by the lowest bottom water oxygen concentrations (Fig. 2g) and the lowest sediment grain-size values (Fig. 2h). The total dinocyst concentrations (Figs. 2c, 3a) and in a lesser extent the specific richness (Fig. 2d) follow the same trend. The 6 m isobath therefore seems to constitute a limit below which dinocyst concentrations are greater.

4.3. Correlation matrix of variables

The correlation matrix of variables (Fig. 4) shows strong correlations between the different variables here used to explain the dinocyst distribution. Among these, a good positive correlation ($r > 0.5$) is noted between ‘Hdino’ and three variables: ‘depth’, ‘granulo<125’ and ‘DeepForam’ (Fig. 4). Heterotrophic dinocysts therefore increase with the bathymetry, in parallel with finer sediments and increasing occurrences of the deepest foraminiferal taxa. Also, a similar correlation with ‘depth’, ‘granulo<125’ and ‘DeepForam’ is observed with ‘Cdino’ and ‘Srdino’ (Fig. 4), likely caused by the greater occurrences of heterotrophics in the deepest zones of the BQ (> 6 m). Finally, a good positive correlation is noted between

‘Srdino’, ‘Cdino’, and to a lesser extent ‘Hdino’, and on the other hand ‘O2’, while ‘Hdino’ is little or not correlated with “Chla” (Fig. 4).

5. Discussion

5.1. Taphonomic issues and dinocyst preservation in the Bay of Quiberon

Some discrepancies in dinocyst distribution are observed within the BQ, especially for the heterotrophic taxa, showing slightly higher occurrences in the deepest areas (below the 6 m bathymetric threshold; Figs. 2e and 3a; Fig. 4). Furthermore, we assume that the small BQ (i.e. 40 km²), characterized by strong tidal currents (cf. gyrotory circulation in Fig. 1) which homogenize surface water properties including nutrients (Tessier, 2006), cannot explain the differential distribution of heterotrophic dinocysts in the BQ (Figs. 2e and 3a). *Brigantedinium* species, which dominate the heterotrophic assemblages (Fig. 3), as well as *Echinidinium* species, are sensitive to oxidation (Zonneveld *et al.*, 1997; Kodrans-Nsiah *et al.*, 2008; Bogus *et al.*, 2014). Their occurrences even decrease logarithmically with increasing bottom water oxygen concentrations (Zonneveld *et al.*, 2001, 2007, 2008). Double-walled organic dinocysts (i.e. dormant resting stages with a mandatory dormancy period; Anderson and Wall, 1978) are composed of a macromolecule, whose chemical composition consists in a cellulose-like glucan in autotrophic, and a nitrogen-rich glycan in heterotrophic forms (Bogus *et al.*, 2014). This difference in dinocyst chemical composition explains the greater vulnerability of heterotrophics to oxidation and a differential preservation during diagenetic processes (Bogus *et al.*, 2014).

In our study, statistical correlation between the percentages of heterotrophic dinocysts and measured environmental parameters allowed us to discuss the significance of the heterotrophic signature in the BQ (Fig. 4). A lack of correlation between ‘Chla’ and ‘Hdino’ ($r = -0.06$; Fig. 4) suggests that productivity is not a main factor explaining differences in the

268 BQ spatial distribution of heterotrophic dinocysts. The weak negative correlation observed
269 between heterotrophic cysts ('Hdino') and 'O₂' ($r = -0.25$; Fig. 4) is mitigated by a non-
270 obvious statistical correlation ($p\text{-value}=0.369$; Fig. 4). Moreover, dissolved oxygen values
271 ('O₂'), are derived from occasional measurements and are not representative of an averaged
272 state of the BQ bottom water oxygenation. Indeed, seasonal hypoxia have been recognized in
273 the deepest areas of the BQ and related to the establishment of a seasonal water column
274 stratification, with oyster mortality below the bathymetric threshold of 6 m (*Stanisière et al.*,
275 2013). Therefore, to test the effect of heterotrophic degradation(/preservation) under
276 oxic(/anoxic) conditions, benthic foraminiferal data have been additionally considered. The
277 deepest benthic foraminiferal assemblage considered ('DeepForam'; Fig. 2f) is mainly
278 constituted by opportunistic species and characterize areas subjected to seasonal hypoxia,
279 confirming the modern environmental assessment (*Stanisière et al.*, 2013). It is also worth
280 noting that the water column stratification, and its effects on the seasonal bottom water
281 oxygen depletion from the 6 m isobath, is also confirmed by i) the negative correlation
282 between 'depth' and 'Temp' ($r = -0.79$; Fig. 4), as well as between 'depth' and 'O₂' ($r = -0.70$;
283 Fig. 4), and ii) the positive correlation between 'depth' and 'DeepForam' ($r = 0.95$; Fig. 4).
284 The positive correlations we observed between 'DeepForam' and 'Hdino' ($r = 0.76$; Fig. 4),
285 'DeepForam' and 'Srdino' ($r = 0.49$; Fig. 4) and 'DeepForam' and 'Cdino' ($r = 0.57$; Fig. 4)
286 therefore suggest that depleted oxygen concentrations may be involved in the higher dinocyst
287 preservation by increasing heterotrophic taxa percentages and dinocyst concentrations. The
288 heterotrophic signature also seems to be correlated with grain-size values. The distribution
289 map (Fig. 2h) and the Pearson correlation coefficient (Fig. 4) show that the proportion of the
290 finest sediments increases with depth. A significant correlation is highlighted between
291 'granulo<125' and 'Hdino' ($r = 0.56$; Fig. 4), 'granulo<125' and 'Srdino' ($r = 0.61$; Fig. 4)
292 and 'granulo<125' and 'Cdino' ($r = 0.75$; Fig. 4). It is well-known that coarser sediments are

not conducive to a good preservation of palynomorphs (cf. example of sampling site n°3 in the BQ; Fig. 3a) due to interstitial fluid circulation and higher oxygenation in a porous sediment. The coarser the sediment, the lower the proportion of heterotrophics (Figs. 2e, h). Variations in the proportions of heterotrophics may thus be related to the effect of oxidation processes acting on species-selective degradation after cyst deposition in the BQ.

A conceptual model allows gathering environmental conditions prevailing in the BQ to explain the differential dinocyst distribution pattern (Fig. 5). At the scale of the study area, we postulate that “autotrophic/heterotrophic” dinocyst fluxes to the sediments are almost identical at all points of the BQ (red arrows on Fig. 5), due to a bay-wide homogenization of sea-surface properties through tidal currents. Beyond 6 m deep, the water column stratification results in an oxygen bottom-water consumption which exceeds its renewal and thus in seasonal bottom-water hypoxia. Because of this stratification, the weakening of coastal and tidal currents in the deepest areas of the BQ enhanced the sedimentation of finer sediments. The combination of seasonal bottom-water oxygen depletion and higher proportion of finer sediments may explain the greater occurrences of heterotrophics below the 6 m isobath.

Such considerations lead us to consider with great caution, in shallow-bay paleoecological reconstructions, the use of heterotrophic-derived productivity indexes. In this context, *Zonneveld et al. (2007)* suggested the use of the absolute concentrations of autotrophic dinocysts rather than total or heterotrophic concentrations to discuss varying productivity conditions. Also, since the sediment granulometry plays a crucial role in the dinocyst preservation, it appears essential to carry out grain-size analyses along core or to work in homogeneous sediment contexts.

5.2. Inshore-Offshore dinocyst assemblages across the Southern Brittany shelf

The influence of environmental parameters on the dinocyst distribution is increasingly understood thanks to the gradual **improvement** of the world marine current databases and atlases (e.g. Zonneveld *et al.*, 2013; Marret *et al.*, 2020; de Vernal *et al.*, 2020; Van Nieuwenhove *et al.*, 2020). However, although the highest dinocyst concentrations are observed in neritic and coastal areas, studies on current dinocyst distributions in French coastal environments are still scarce (e.g. Morzadec-Kerfourn, 1977; Larrazabal *et al.*, 1990; Ganne *et al.*, 2016; Lambert *et al.*, 2017). From previous studies (e.g. Williams, 1971; Morzadec-Kerfourn, 1977; Penaud *et al.*, 2020), dinocyst groups have been established: i) the oceanic zone (>100-150 m water depth, outer-neritic assemblage) appears characterized by ***Impagidinium*** *aculeatum*, *O. centrocarpum*, *S. mirabilis*, and *S. elongatus* (with *S. ramosus* and *S. bulloideus* in addition), *I. aculeatum* being restricted to full-oceanic waters, ii) the coastal zone (inner-neritic) is characterized by the association *S. ramosus*-*S. bulloideus*-*S. bentorii*, and iii) the estuarine-coastal zone, under fluvial-derived major influence, is characterized by *L. machaerophorum*, a species tolerant to large drops in salinity and mainly proliferating in brackish environments (Reid, 1975; Morzadec-Kerfourn, 1977, 1997; **Mudie *et al.*, 2017**; Penaud *et al.*, 2020).

Along the inshore-offshore gradient (Fig. 6a), estuarine to inner-neritic samples under strong fluvial influences exhibit an almost monospecific assemblage of *L. machaerophorum* (more than 80 %; Fig. 6b). *L. machaerophorum* is becoming less and less abundant with the distance from the coast and is rarely observed in the full-oceanic environment (i.e. around 0.3% in the MD95-2002 core; Fig. 6b). The offshore **sea-surface** conditions are indeed influenced by the North Atlantic general circulation, while the circulation on the continental shelf is influenced

by a mixed river / tidal current limited to the coast (Penaud et al., 2020). In shelf sediments (CBT-CS11 and VK03-58bis cores), the prevalence of the *L. machaerophorum* species over neritic to oceanic cyst taxa thus suggests seasonally coastal stratified waters subjected to strong continental influence (Penaud et al., 2020). Indeed, from mid-autumn to early spring, strong river flows (i.e. Gironde, Loire, Vilaine) associated with sustained northeastward wind activity maintain this region under the influence of northward freshwater plumes and associated low salinities between the coast and the 100 m isobath (Lazure et al., 2008; Charria et al., 2013; Costoya et al., 2015, 2016). The resulting density gradients explain water mass stratification and thermohaline front at the 100 m isobath, and thus the prevalence of *L. machaerophorum* until this limit (Penaud et al., 2020).

The transect confirms the ecological preferences of *S. bentorii* and *S. ramosus* for the coastal environments. However, while *S. bentorii* seems to be a good marker of the strict proximal domain (i.e. strong occurrence in BQ: 11.5 %; Fig. 6b), being almost absent from the shelf (i.e. VK03-58bis and CBT-CS11 cores: 0.3 and 2 %, respectively), *S. ramosus* exhibits an inverse distribution and becomes more and more present away from the coast (Fig. 6b): *S. ramosus* reaches 5% in the full-oceanic domain (MD95-2002 core) while *S. bentorii* is totally absent. *S. ramosus* and *S. bentorii* can therefore be considered as excellent markers of the proximal neritic environment under moderate fluvial influences. Cysts of *P. dalei* show a fairly homogeneous distribution and low percentages all along the transect (i.e. 3 to 10%; Fig. 6b), being more dominant in northern latitudes of the North Atlantic Ocean and in fjords (Mudie and Rochon, 2001; Zonneveld et al., 2013; Heikkilä et al., 2014; Marret et al., 2020). This species also occurs in environments where upper water salinities are reduced as a result of meltwater or river inputs (Zonneveld et al., 2013). The neritic zone of the southern Brittany shelf, marked by a winter salinity front, may explain its greater occurrence in the proximal zone of the continental shelf (i.e. CBT-CS11 and BQ; 12 % and 5 %, respectively). In

temperate waters, cysts of *P. dalei* may likely be used as indicators of cooling and/or continental influences. *S. mirabilis* and *O. centrocarpum* are not significant in the Loire Estuary and in the other three coastal sites (i.e. BQ, CBT-CS11 and VK03-58bis; Fig. 6b), whereas both taxa respectively reach 53 and 21% in the deepest site (i.e. MD95-2002; Fig. 6b). These results confirm their affinity for full-oceanic North Atlantic areas. The distribution of heterotrophic dinocysts along this transect is more difficult to interpret. Although we cannot exclude an influence of productivity conditions on heterotrophics, their virtual absence from the Loire Estuary (LE; Fig. 6b) raises questions as it is the most productive area of the transect (Gohin *et al.*, 2019). As previously mentioned in section 5.1, conditions of oxygenation may result in differences between heterotrophic preservation. Comparing heterotrophics would also require to consider mean bottom oxygen conditions and grain-size values for each analyzed site.

6. Conclusion

The Bay of Quiberon (BQ), characterized by seasonal hypoxia, appears appropriate to investigate the effects of the different degrees of bottom water oxygenation on dinocyst taphonomic processes (i.e. species-selective degradation after cyst deposition). Among dinocyst assemblages, heterotrophic taxa, well-known to be sensitive to degradation processes, here show a spatial distribution that appears mainly controlled by bottom-water oxygen conditions and sediment granulometry; lower heterotrophic percentages and dinocyst diversity are observed under “higher O₂-coarser sediments”. Heterotrophic occurrences in coastal sediments are here mainly associated to oxidation processes, leading to caution about their use as productivity indexes in paleoecological reconstructions carried out in these kinds

of shallow environments, unless high-resolution grain-size analyses are at least conducted in parallel with palynological studies to avoid misinterpretations.

The comparison of the averaged dinocyst results acquired in the BQ with surface sediments and top cores, issued from already published data, made it possible to improve our knowledge regarding the dinocyst distribution along a northern Bay of Biscay (southern Brittany) inshore-offshore gradient. We highlighted clear different ecological groups according to the hydrological and bathymetric contexts: i) an estuarine assemblage at the outlet of the Loire river strongly dominated by *L. machaerophorum*, ii) a proximal coastal assemblage in the shallow BQ still dominated by *L. machaerophorum* with, to a lesser extent, *S. bentorii* and *S. membranaceus*, iii) a neritic assemblage dominated by *L. machaerophorum*, *S. ramosus* and cysts of *P. dalei*, and iv) an oceanic group dominated by *S. mirabilis* and *O. centrocarpum* and in which *L. machaerophorum* is rare or absent.

7. Acknowledgment

The sediment sample collect as well as the environmental parameter measurements were carried out within the framework of the RISCO project (2010-2013; coord: J. Mazurié) coordinated by the ‘Comité régional de la conchyliculture Bretagne Sud’, labeled ‘Pôle Mer Bretagne’ and set up jointed by the ‘Laboratoire Environnement Ressources’ (Ifremer). RISCO project was funded by the ‘Conseil Régional de Bretagne’. Analysis also benefited credits by a CNRS-INSU project HCOG2 ‘Forçages climatiques Holocène et répercussions Côtières et Océaniques dans le Golfe de Gascogne’ (2013-2014 ; coord. A. Penaud) in the context of the LEFE-IMAGO research axis.

8. Data availability

The dinocyst dataset related to this article (dinocyst counts on the 15 samples collected in the Bay of Quiberon) can be found in the supplementary material.

9. Declaration of competing interest

The authors declare that they have no competing interests.

10. References

Baltzer, A., Walter-Simonnet, A. V., Mokeddem, Z., Tessier, B., Goubert, E., Cassen, S.,
Diffio, A., 2014. Climatically-driven impacts on sedimentation processes in the Bay of
Quiberon (south Brittany, France) over the last 10,000 years. *The Holocene*, 24(6), 679-688.

Bogus, K., Mertens, K. N., Lauwaert, J., Harding, I. C., Vrielinck, H., Zonneveld, K. A.,
Versteegh, G. J., 2014. Differences in the chemical composition of organic-walled
dinoflagellate resting cysts from phototrophic and heterotrophic dinoflagellates. *Journal of
Phycology*, 50(2), 254-266.

Charria, G., Lazure, P., Le Cann, B., Serpette, A., Reverdin, G., Louazel, S., Batifoulier, F.,
Dumas, F., Pichon, A., Morel, Y., 2013. Surface layer circulation derived from Lagrangian
drifters in the Bay of Biscay. *Journal of Marine Systems*, 109, S60-S76.

Costoya, X., Decastro, M., Gómez-Gesteira, M., Santos, F., 2015. Changes in sea surface
temperature seasonality in the Bay of Biscay over the last decades (1982–2014). *Journal of
Marine Systems*, 150, 91-101.

433 Costoya, X., Fernández-Nóvoa, D., Decastro, M., Santos, F., Lazure, P., Gómez-Gesteira, M.,
434 2016. Modulation of sea surface temperature warming in the Bay of Biscay by Loire and
435 Gironde Rivers. *Journal of Geophysical Research: Oceans*, 121(1), 966-979.

436 Dale, B., 1996. Dinoflagellate cyst ecology: modeling and geological applications. In:
437 Jansonius, J., McGregor, D.C. (Eds.), *Palynology: Principles and Applications*. American
438 Association of Stratigraphic Palynologists Foundation, Dallas, pp. 1249–1276.

439 Dale, B., Thorsen, T. A., Fjellsa, A., 1999. Dinoflagellate cysts as indicators of cultural
440 eutrophication in the Oslofjord, Norway. *Estuarine, Coastal and Shelf Science*, 48(3), 371-
441 382.

442 de Vernal, A., Henry, M., Bilodeau, G., 1999. Techniques de préparation et d'analyse en
443 micropaléontologie. *Les cahiers du GEOTOP*, 3, 41.

444 de Vernal, A., Hillaire-Marcel, C., Rochon, A., Fréchette, B., Henry, M., Solignac, S.,
445 Bonnet, S., 2013. Dinocyst-based reconstructions of sea ice cover concentration during the
446 Holocene in the Arctic Ocean, the northern North Atlantic Ocean and its adjacent seas.
447 *Quaternary Science Reviews*, 79, 111-121.

448 de Vernal, A., Radi, T., Zaragosi, S., Van Nieuwenhove, N., Rochon, A., Allan, E., De
449 Schepper, S., Eynaud, F., Head, M. J., Limoges, A., Londeix, L., Marret, F., Matthiessen, J.,
450 Penaud, A., Pospelova, V., Price, A., Richerol, T., 2020. Distribution of common modern
451 dinoflagellate cyst taxa in surface sediments of the Northern Hemisphere in relation to
452 environmental parameters: The new n= 1968 database. *Marine Micropaleontology*, 159,
453 101796.

454 Dodge, J. D., Harland, R., 1991. The distribution of planktonic dinoflagellates and their cysts
455 in the eastern and northeastern Atlantic Ocean. *New Phytologist*, 118(4), 593-603.

456 Evitt, W. R., 1985. *Sporopollenin Dinoflagellate Cysts: Their Morphology and Interpretation*.
457 American Association of Stratigraphic Palynologists Foundation, Austin, Te. USA.

458 Fatela, F., Taborda, R., 2002. Confidence limits of species proportions in microfossil
459 assemblages. *Marine Micropaleontology*, 45(2), 169-174.

460 Ganne, A., Leroyer, C., Penaud, A., Mojtahid, M., 2016. Present-day palynomorph deposits in
461 an estuarine context: The case of the Loire Estuary. *Journal of Sea Research*, 118, 35-51.

462 García-Moreiras, I., Pospelova, V., García-Gil, S., Sobrino, C. M., 2018. Climatic and
463 anthropogenic impacts on the Ría de Vigo (NW Iberia) over the last two centuries: A high-
464 resolution dinoflagellate cyst sedimentary record. *Palaeogeography, Palaeoclimatology,*
465 *Palaeoecology*, 504, 201-218.

466 Gohin, F., Van der Zande, D., Tilstone, G., Eleveld, M. A., Lefebvre, A., Andrieux-Loyer, F.,
467 Blauw, A. N., Bryère, P., Devreker, D., Garnesson, P., Hernandez Fariñas, T., Lamaury, Y.,
468 Lampert, L., Lavigne, H., Menet-Nedelec, F., Pardo, S., Saulquin, B., 2019. Twenty years of
469 satellite and in situ observations of surface chlorophyll-a from the northern Bay of Biscay to
470 the eastern English Channel. Is the water quality improving?. *Remote Sensing of*
471 *Environment*, 233, 111343.

472 Gómez, F., 2012. A quantitative review of the lifestyle, habitat and trophic diversity of
473 dinoflagellates (Dinoflagellata, Alveolata). *Systematics and Biodiversity*, 10(3), 267-275

474 Hallegraeff, G. M., 1995. Harmful algal blooms: a global overview, p. 1–22. In G. M.
 475 Hallegraeff, D. M. Anderson, and A. D. Cembella (ed.), Manual on harmful marine
 476 microalgae. UNESCO, Paris, France.

477 Hammer, Ø., Harper, D. A., Ryan, P. D., 2001. PAST: Paleontological statistics software
 478 package for education and data analysis. *Palaeontologia electronica*, 4(1), 9.

479 Hardy, W., Marret, F., Penaud, A., Le Mezo, P., Droz, L., Marsset, T., Kageyama, M., 2018.
 480 Quantification of last glacial-Holocene net primary productivity and upwelling activity in the
 481 equatorial eastern Atlantic with a revised modern dinocyst database. *Palaeogeography*,
 482 *Palaeoclimatology, Palaeoecology*, 505, 410-427.

483 Heikkilä, M., Pospelova, V., Hochheim, K. P., Kuzyk, Z. Z. A., Stern, G. A., Barber, D. G.,
 484 Macdonald, R. W., 2014. Surface sediment dinoflagellate cysts from the Hudson Bay system
 485 and their relation to freshwater and nutrient cycling. *Marine Micropaleontology*, 106, 79-109.

486 Kodrans-Nsiah, M., de Lange, G. J., Zonneveld, K. A., 2008. A natural exposure experiment
 487 on short-term species-selective aerobic degradation of dinoflagellate cysts. *Review of*
 488 *Palaeobotany and Palynology*, 152(1-2), 32-39.

489 Lambert, C., Vidal, M., Penaud, A., Combourieu-Nebout, N., Lebreton, V., Ragueneau, O.,
 490 Gregoire, G., 2017. Modern palynological record in the Bay of Brest (NW France): Signal
 491 calibration for palaeo-reconstructions. *Review of Palaeobotany and Palynology*, 244, 13-25.

492 Larrazabal, M. E., Lassus, P., Maggi, P., Bardouil, M., 1990. Kystes modernes de
 493 dinoflagellés en baie de Vilaine-Bretagne sud (France). *Cryptogamie, Algologie*, 11(3), 171-
 494 185.

495 Lassus, P., Chomerat, N., Hess, P., Nezan, E., 2016. Toxic and Harmful Microalgae of the
 496 World Ocean. IOC Manuals and Guides, 68.

497 Lazure, P., Dumas, F., Vrignaud, C., 2008. Circulation on the Armorican shelf (Bay of
 498 Biscay) in autumn. Journal of Marine systems, 72(1-4), 218-237.

499 Lemoine, G., 1989. Étude sédimentaire de la Baie de Quiberon : la zone ostréicole en eau
 500 profonde et ses abords. Rapport de stage. <https://archimer.ifremer.fr/doc/00000/2210/>

501 Marret, F., Zonneveld, K. A., 2003. Atlas of modern organic-walled dinoflagellate cyst
 502 distribution. Review of Palaeobotany and Palynology, 125(1-2), 1-200.

503 Marret, F., Bradley, L., de Vernal, A., Hardy, W., Kim, S. Y., Mudie, P., Penaud, A.,
 504 Pospelova, V., Price, A. M., Radi, T., Rochon, A., 2020. From bi-polar to regional
 505 distribution of modern dinoflagellate cysts, an overview of their biogeography. Marine
 506 Micropaleontology, 159, 101753.

507 Matsuoka, K., 1999. Eutrophication process recorded in dinoflagellate cyst assemblages - a
 508 case of Yokohama Port, Tokyo Bay, Japan. Science of the Total Environment, 231(1), 17-35.

509 Mazurié, J., Stanisiere, J. Y., Langlade, A., Bouget, J. F., Dumas, F., Treguier, C., Leclerc, E.,
 510 Ravaud, E., Quinsat, K., Gabellec, R., Retho, M., Cochet, H., Dreano, A., 2013b. *Les risques*
 511 *conchylicoles en Baie de Quiberon. Première partie : le risque de mortalité virale du naissain*
 512 *d'huître creuse Crassostrea gigas*. Rapport final du projet Risco 2010-2013.
 513 RST/LER/MPL/13.19.

514 Mazurié, J., Stanisiere, J. Y., Bouget, J. F., Langlade, A., Leclerc, E., Quinsat, K., Herve, G.,
 515 Augustin, J. M., Ehrhold, A., Siquin, J. M., Meidi-Deviarni, I., Goubert, E., Cochet, H.,

516 Dreano, A., 2013b. *Les risques conchyliques en Baie de Quiberon. Deuxième partie : le*
517 *risque de prédation sur l'huître creuse Crassostrea gigas*. Rapport final du projet Risco 2010-
518 2013. RST/LER/MPL/13-20.

519 Menier, D., Augris, C., Briend, C., 2014. *Les réseaux fluviaux anciens du plateau*
520 *continental de Bretagne Sud*. Editions Quae, p 104.

521 Mertens, K. N., Verhoeven, K., Verleye, T., Louwye, S., Amorim, A., Ribeiro, S., Deaf, A.
522 S., Harding, I. C., De Schepper, S., Gonzalez, C., Kodrans-Nsiah, M., de Vernal, A., Henry,
523 M., Radi, T., Dybkjaer, K., Poulsen, N. E., Feist-Burkhardt, S., Chitolie, J., Heilmann-
524 Clausen, C., Londeix, L., Turon, J. L., Marret, F., Matthiessen, J., McCarthy, F. M. G.,
525 Prasad, V., Pospelova, V., Kyffin Hughes, J. E., Riding, J. B., Rochon, A., Sangiorgi, F.,
526 Welters, N., Sinclair, N., Thun, C., Soliman, A., Van Nieuwenhove, N., Vink, A., Young, M.,
527 2009. Determining the absolute abundance of dinoflagellate cysts in recent marine sediments:
528 the Lycopodium marker-grain method put to the test. *Review of Palaeobotany and*
529 *Palynology*, 157(3-4), 238-252.

530 Morzadec-Kerfourn, M. T., 1977. Les Kystes de dinoflagellés dans les sédiments récents le
531 long des côtes Bretonnes. *Revue de Micropaléontologie*, 20, 157-66.

532 Morzadec-Kerfourn, M. T., 1997. Dinoflagellate cysts and the paleoenvironment of Late-
533 Pliocene early-pleistocene deposits of Brittany, Northwest France. *Quaternary Science*
534 *Reviews*, 16(8), 883-898.

535 Mudie, P.J., Harland, R., Matthiessen, J., de Vernal, A., 2001. Dinoflagellate cysts and high
536 latitude Quaternary paleoenvironmental reconstructions: an introduction. *Journal of*
537 *Quaternary Science*, 16, 595–602.

538 Mudie, P. J., Rochon, A., 2001. Distribution of dinoflagellate cysts in the Canadian Arctic
539 marine region. *Journal of Quaternary Science: Published for the Quaternary Research*
540 *Association*, 16(7), 603-620.

541 Mudie, P. J., Marret, F., Mertens, K. N., Shumilovskikh, L., Leroy, S. A., 2017. Atlas of
542 modern dinoflagellate cyst distributions in the Black Sea Corridor: from Aegean to Aral Seas,
543 including Marmara, Black, Azov and Caspian Seas. *Marine Micropaleontology*, 134, 1-152.

544 Naughton, F., Bourillet, J. F., Sánchez Goñi, M. F., Turon, J. L., Jouanneau, J. M., 2007.
545 Long-term and millennial-scale climate variability in northwestern France during the last
546 8850 years. *The Holocene*, 17(7), 939-953.

547 Penaud, A., Eynaud, F., Voelker, A. H. L., Turon, J. L., 2016. Palaeohydrological changes
548 over the last 50 ky in the central Gulf of Cadiz: complex forcing mechanisms mixing multi-
549 scale processes. *Biogeosciences*, 13(18), 5357-5377.

550 Penaud, A., Ganne, A., Eynaud, F., Lambert, C., Coste, P. O., Herlédan, M., Vidal, M.,
551 Goslin, J., Stéphan, P., Charria, G., Paillet, Y., Durand, M., Zumaque, J., Mojtahid, M., 2020.
552 Oceanic versus continental influences over the last 7 kyrs from a mid-shelf record in the
553 northern Bay of Biscay (NE Atlantic). *Quaternary Science Reviews*, 229, 106135.

554 Pospelova, V., Kim, S. J., 2010. Dinoflagellate cysts in recent estuarine sediments from
555 aquaculture sites of southern South Korea. *Marine Micropaleontology*, 76(1-2), 37-51.

556 Price, A. M., Coffin, M. R., Pospelova, V., Latimer, J. S., Chmura, G. L., 2017. Effect of
557 nutrient pollution on dinoflagellate cyst assemblages across estuaries of the NW Atlantic.
558 *Marine pollution bulletin*, 121(1-2), 339-351.

559 Price, A. M., Baustian, M. M., Turner, R. E., Rabalais, N. N., Chmura, G. L., 2018.
560 Dinoflagellate cysts track eutrophication in the Northern Gulf of Mexico. *Estuaries and*
561 *Coasts*, 41(5), 1322-1336.

562 Radi, T., de Vernal, A., 2004. Dinocyst distribution in surface sediments from the
563 northeastern Pacific margin (40–60 N) in relation to hydrographic conditions, productivity
564 and upwelling. *Review of Palaeobotany and Palynology*, 128(1-2), 169-193.

565 Reid, P. C., 1972. Dinoflagellate cyst distribution around the British Isles. *Journal of the*
566 *Marine Biological Association of the United Kingdom*, 52(4), 939-944.

567 Reid, P. C., 1975. A regional sub-division of dinoflagellate cysts around the British Isles.
568 *New Phytologist*, 75(3), 589-603.

569 Rochon, A., Vernal, A. D., Turon, J. L., Matthiessen, J., Head, M. J., 1999. Distribution of
570 recent dinoflagellate cysts in surface sediments from the North Atlantic Ocean and adjacent
571 seas in relation to sea-surface parameters. *American Association of Stratigraphic*
572 *Palynologists Contribution Series*, 35, 1-146.

573 Sangiorgi, F., Donders, T. H., 2004. Reconstructing 150 years of eutrophication in the north-
574 western Adriatic Sea (Italy) using dinoflagellate cysts, pollen and spores. *Estuarine, Coastal*
575 *and Shelf Science*, 60(1), 69-79.

576 Stanisière J. Y., Mazurié J., Bouget J. F., Langlade A., Gabellec R., Retho M., Quinsat K.,
577 Leclerc E., Cugier P., Dussauze M., Menesguen A., Dumas F., Gohin F., Augustin J. M.,
578 Ehrhold A., Sinquin J. M., Goubert E., Dreano A., 2013. *Les risques conchylicoles en Baie de*

579 *Quiberon. Troisième partie : le risque d'hypoxie pour l'huître creuse Crassostrea gigas.*
580 Rapport final du projet Risco 2010-2013. RST/LER/MPL/13.21.

581 Stockmarr, J. A., 1971. Tabletes with spores used in absolute pollen analysis. Pollen spores,
582 13, 615-621.

583 Taylor F. J. R., 1987. *The Biology of Dinoflagellates*. Blackwell Scientific, Oxford, 785 pp.

584 Tessier, C., 2006. *Caractérisation et dynamique des turbidités en zone côtière : l'exemple de*
585 *la région marine Bretagne Sud*. Doctoral dissertation, University of Bordeaux, France, 428
586 pp.

587 Vanney, J. R., 1965. Étude sédimentologique du Mor Bras, Bretagne. *Marine Geology*, 3(3),
588 195-222.

589 Van Nieuwenhove, N., Head, M. J., Limoges, A., Pospelova, V., Mertens, K. N., Matthiessen,
590 J., De Schepper, S., de Vernal, A., Eynaud, F., Londeix, L., Marret, F., Penaud, A., Radi, T.,
591 Rochon, A., 2020. An overview and brief description of common marine organic-walled
592 dinoflagellate cyst taxa occurring in surface sediments of the Northern Hemisphere. *Marine*
593 *Micropaleontology*, 159, 101814.

594 Von Stosch, H. A., 1973. Observations on vegetative reproduction and sexual life cycles of
595 two freshwater dinoflagellates, *Gymnodinium pseudopalustre* Schiller and *Woloszynskia*
596 *apiculate* sp. nov. *British Phycological Journal*, 8, 105–134.

597 Wall, D., Dale, B., Lohman, G.P., Smith, W.K., 1977. The environmental and climatic
598 distribution of dinoflagellate cysts in the North and South Atlantic Oceans and adjacent seas.
599 *Marine Micropaleontology*. 2, 121-20.

600 Williams, D. B., 1971. The distribution of marine dinoflagellates in relation to physical and
601 chemical conditions. In *The micropalaeontology of oceans* (pp. 91-95). Cambridge University
602 Press Cambridge.

603 Zonneveld, K. A., Versteegh, G. J., de Lange, G. J., 1997. Preservation of organic-walled
604 dinoflagellate cysts in different oxygen regimes: a 10,000-year natural experiment. *Marine*
605 *micropaleontology*, 29(3-4), 393-405.

606 Zonneveld, K. A., Versteegh, G. J., de Lange, G. J., 2001. Palaeoproductivity and post-
607 depositional aerobic organic matter decay reflected by dinoflagellate cyst assemblages of the
608 Eastern Mediterranean S1 sapropel. *Marine Geology*, 172(3-4), 181-195.

609 Zonneveld, K. A., Bockelmann, F., Holzwarth, U., 2007. Selective preservation of organic-
610 walled dinoflagellate cysts as a tool to quantify past net primary production and bottom water
611 oxygen concentrations. *Marine Geology*, 237(3-4), 109-126.

612 Zonneveld, K. A., Versteegh, G., Kodrans-Nsiah, M., 2008. Preservation and organic
613 chemistry of Late Cenozoic organic-walled dinoflagellate cysts: A review. *Marine*
614 *Micropaleontology*, 68(1-2), 179-197.

615 Zonneveld, K. A., Marret, F., Versteegh, G. J., Bogus, K., Bonnet, S., Bouimetarhan, I.,
616 Crouch, E., de Vernal, A., Elshanawany, A., Edwards, L., Esper, O., Forke, S., Grøsfjeld, K.,
617 Henry, M., Holzwarth, U., Kielt, J. F., Kim, S. Y., Ladouceur, S., Ledu, D., Chen, L.,
618 Limoges, A., Londeix, L., Lu, S. H., Mahmoud, M. S., Marino, G., Matsuoka, K.,
619 Matthiessen, J., Mildenhall, D. C., Mudie, P., Neil, H. L., Pospelova, V., Qi, Y., Radi, T.,
620 Richerol, T., Rochon, A., Sangiorgi, F., Solignac, S., Turon, J. L., Verleye, T., Wang, Y.,

621 Wang, Z., Young, M., 2013. Atlas of modern dinoflagellate cyst distribution based on 2405
622 data points. *Review of Palaeobotany and Palynology*, 191, 1-197.

623 Zonneveld, K. A., Pospelova, V., 2015. A determination key for modern dinoflagellate cysts.
624 *Palynology*, 39(3), 387-409.

625 Zumaque, J., Eynaud, F., de Vernal, A., 2017. Holocene paleoceanography of the Bay of
626 Biscay: evidence for West-East linkages in the North Atlantic based on dinocyst data.
627 *Palaeogeography, Palaeoclimatology, Palaeoecology*, 468, 403-413.

628

629

630

631

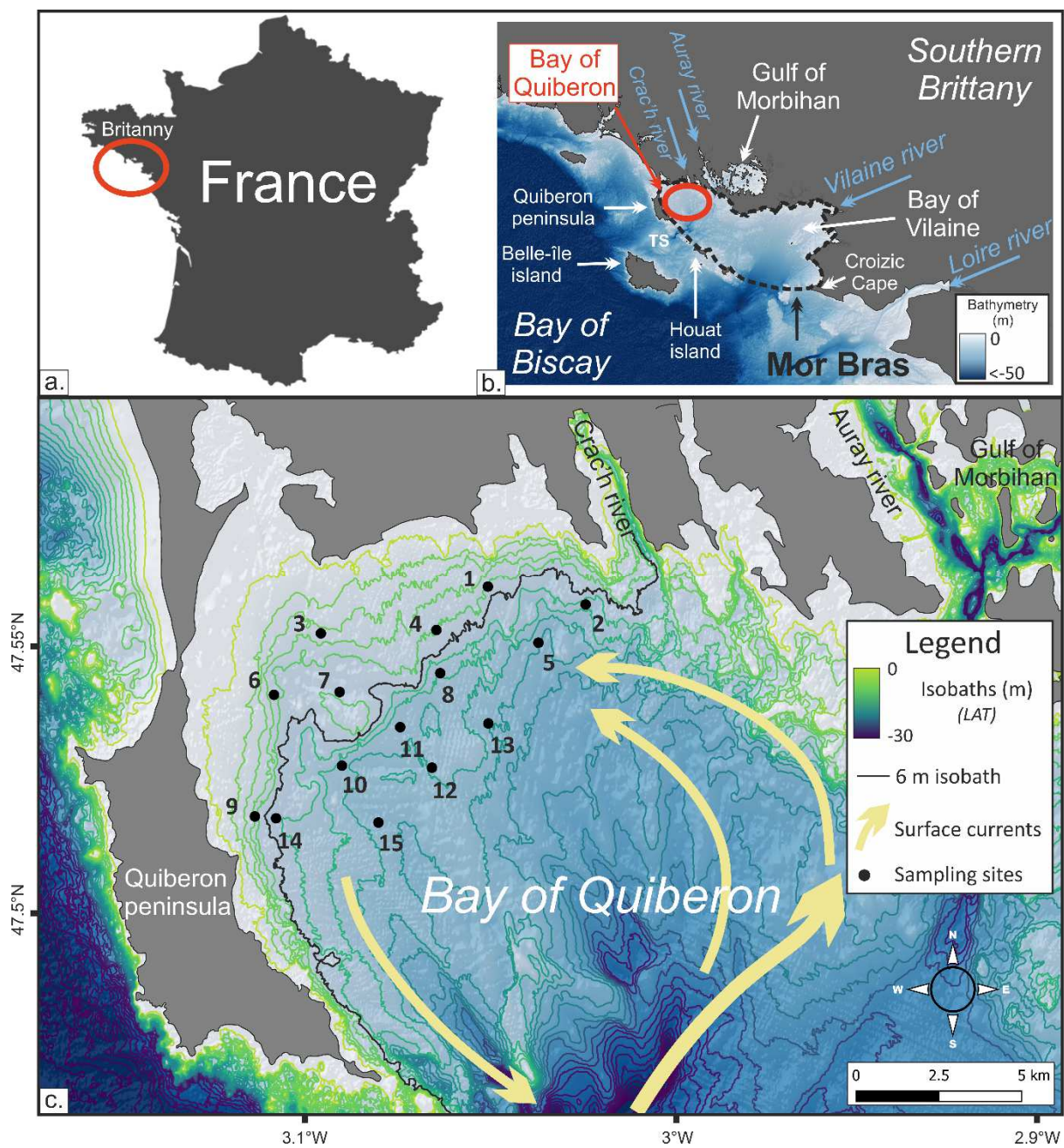
632

633

634

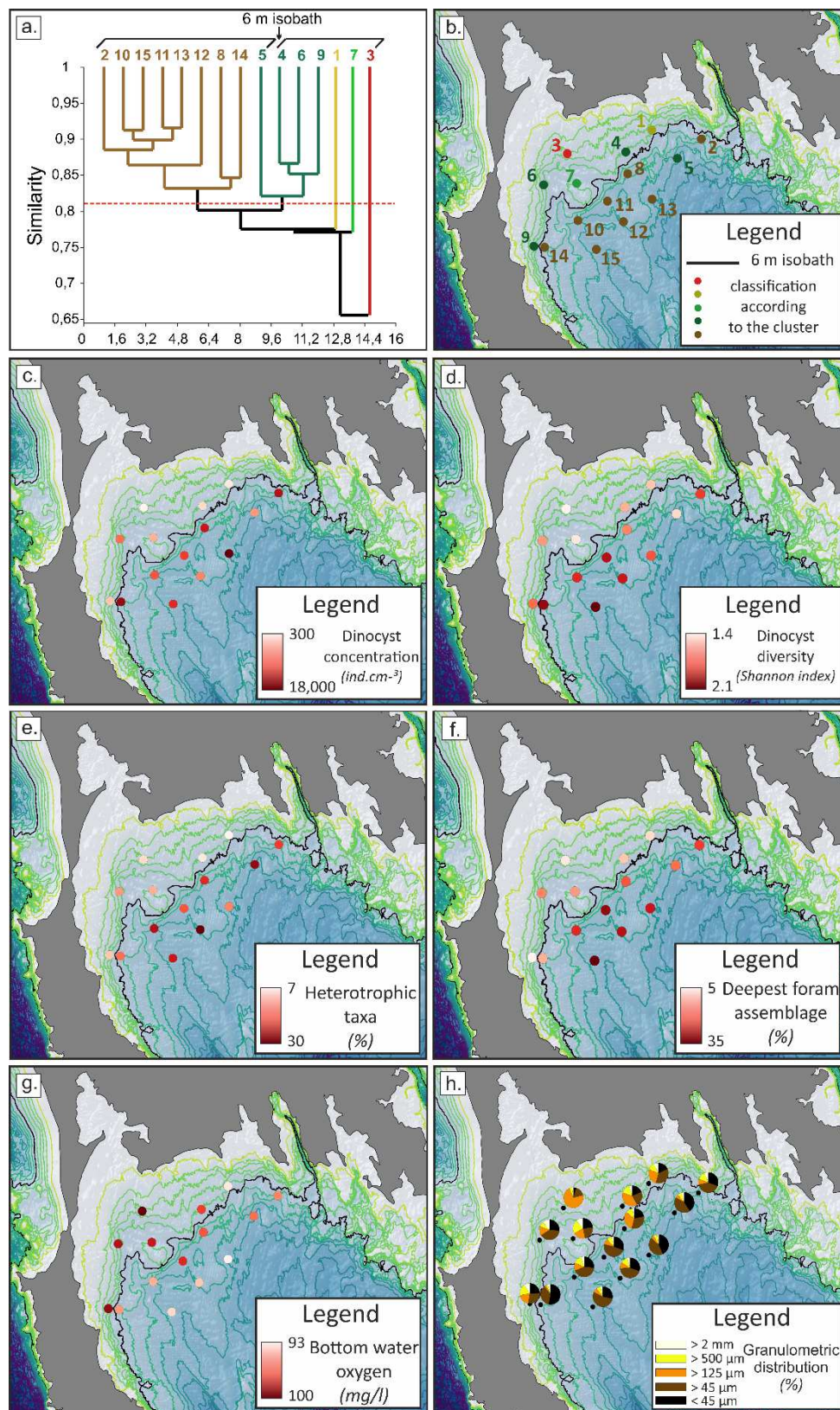
635

636



638

639 **Figure 1**



640

641 Figure 2

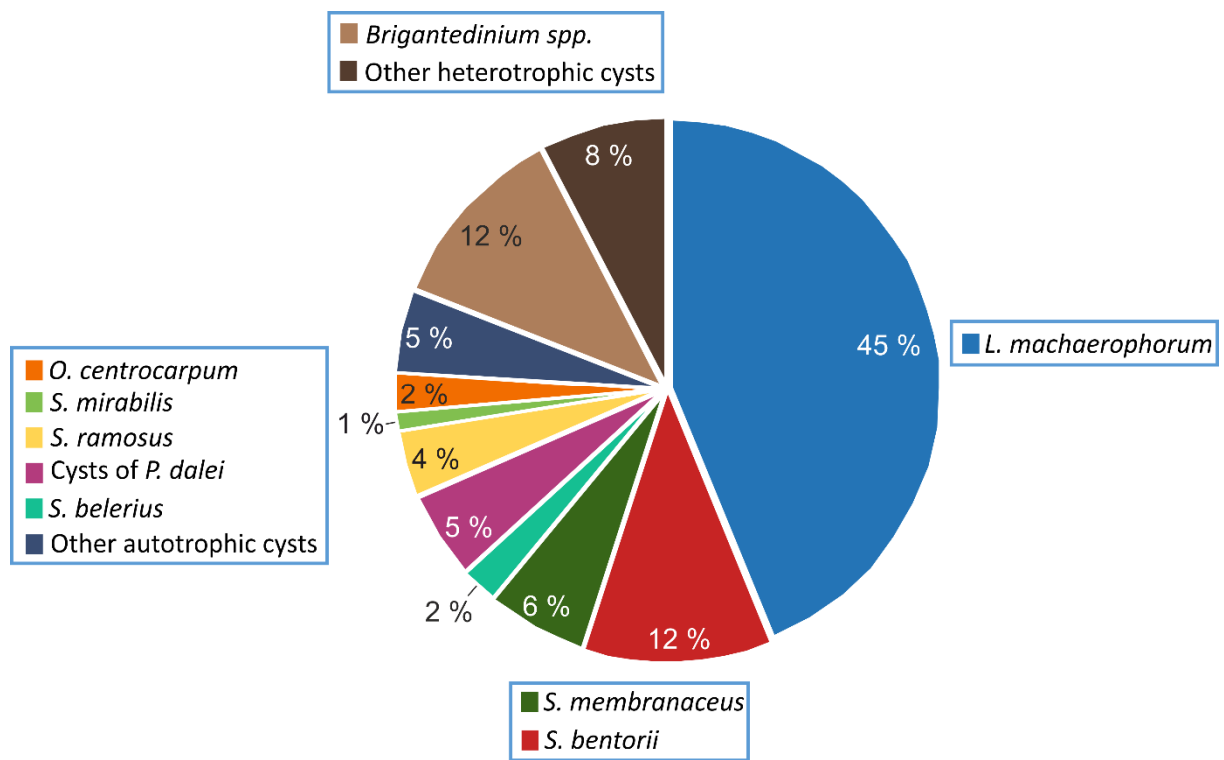
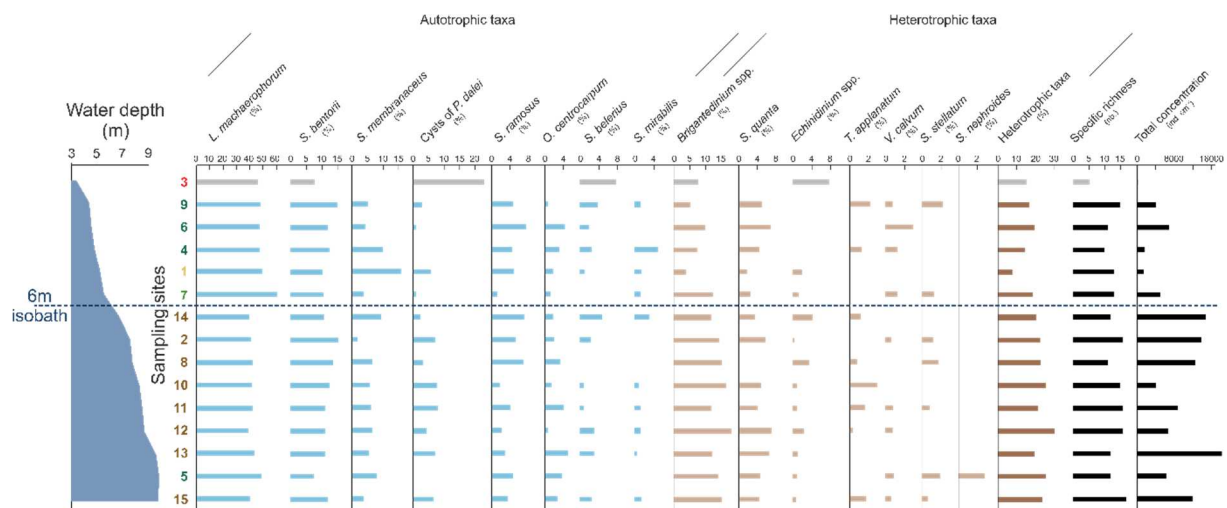


Figure 3

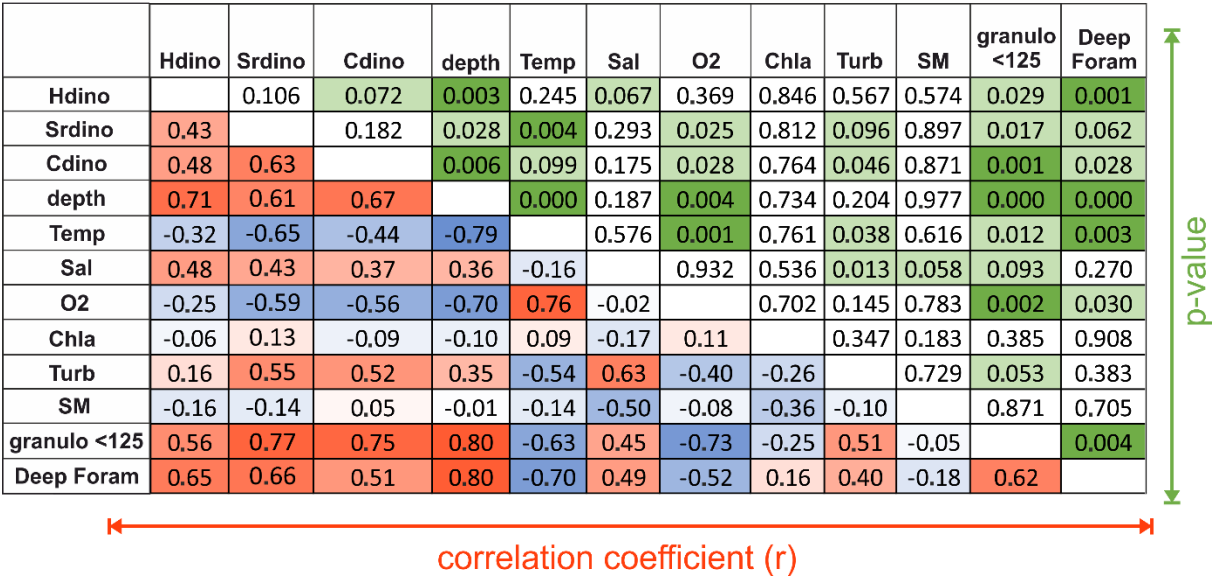


Figure 4

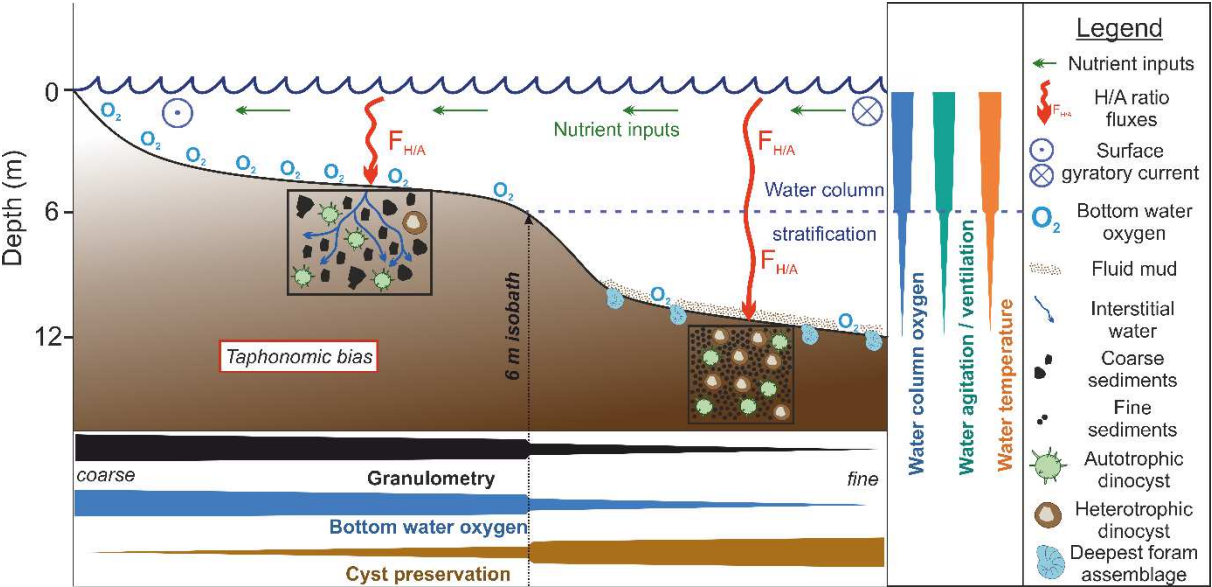


Figure 5:

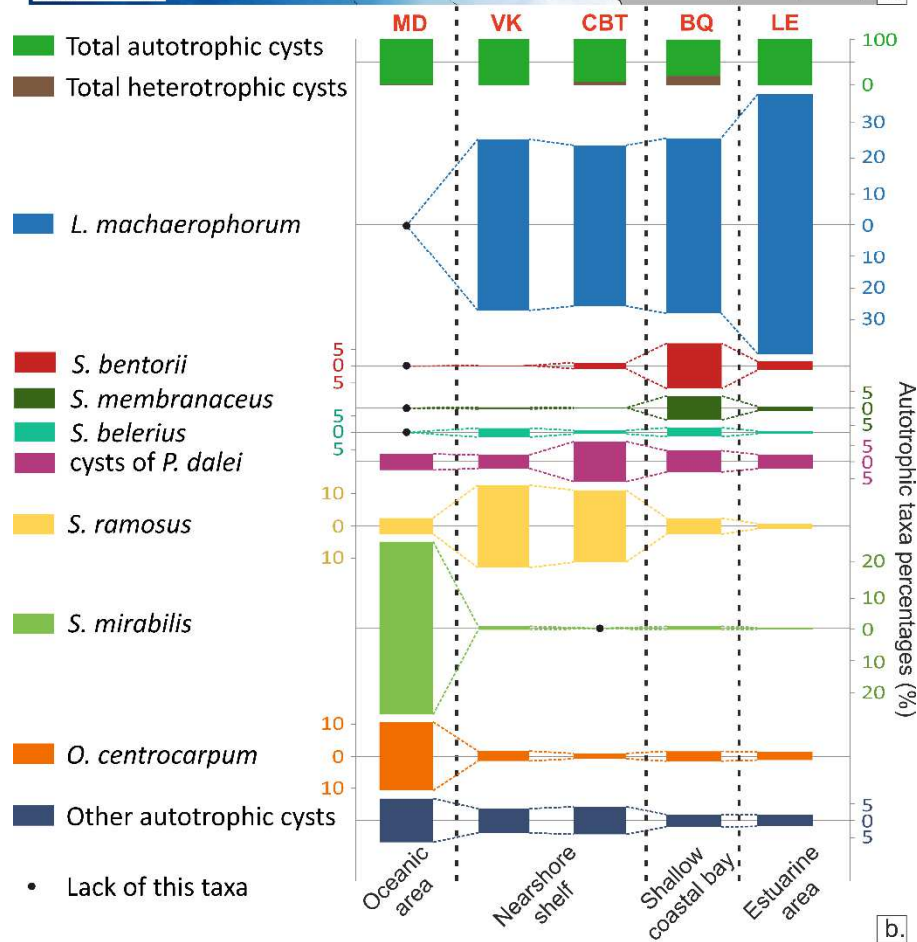
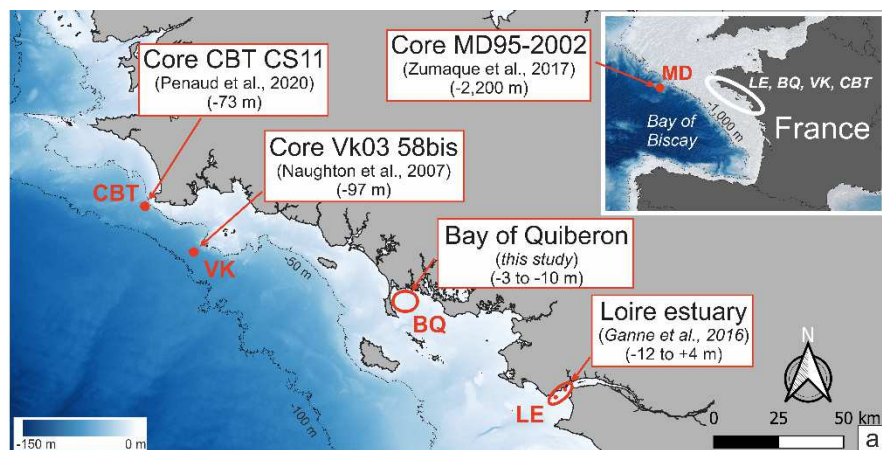


Figure 6

Site	Longitude	Latitude	Sampling depth (m)
1	-3.0501	47.5592979	5.24
2	-3.02359375	47.5560063	7.57
3	-3.09542143	47.5507071	3.37
4	-3.06407917	47.5513313	4.82
5	-3.03639167	47.5489833	9.83
6	-3.10814524	47.5394214	4.58
7	-3.09032917	47.5399396	5.55
8	-3.0630375	47.5434083	7.77
9	-3.11331927	47.5170971	4.4
10	-3.08969323	47.5264333	8.3
11	-3.0739	47.5334896	8.52
12	-3.06528125	47.52605	8.69
13	-3.04997917	47.5341708	9.6
14	-3.10756875	47.5167521	6.75
15	-3.07979245	47.5159747	9.74

655 Table 1

Site	depth (m)	Srdino	Cdino (nb./cm ³)	Hdino (%)	Temp (°C)	Sal (‰)	O2 (mg/l)	Chla (µg/l)	Turb (NTU)	SM (mg/l)	DeepF oram (%)	granulo <125 (%)
1	5.24	1.78	1504.49	7.6	14.5	34.3	93.55	1.95	2.04	6.23	6	54
2	7.57	1.94	13979.95	22.7	14.5	34.4	94.77	1.56	2.40	7.06	12	72

3	3.37	1.48	332.14	15.4	14.8	34.5	100.53	1.94	1.77	5.34	5	21
4	4.82	1.78	1704.96	14.6	14.6	34.4	95.56	1.94	2.09	4.16	8	42
5	9.83	1.77	6313.97	25.9	14.5	34.5	94.84	1.48	1.97	5.29	17	84
6	4.58	1.84	6949.33	19.4	14.7	34.5	96.31	1.89	2.30	4.51	8	66
7	5.55	1.53	5066.16	18.2	14.7	34.5	96.09	1.76	2.03	4.62	10	47
8	7.77	1.87	12657.71	22.7	14.6	34.4	95.25	2.23	1.81	5.17	14	54
9	4.4	1.93	4067.19	16.5	14.6	34.6	97.84	1.81	2.80	4.68	6	52
10	8.3	1.96	8749.84	25.3	14.5	34.5	94.58	2.11	2.17	4.02	14	67
11	8.52	2.03	8831.44	21.3	14.5	34.5	96.02	2.22	2.06	4.63	17	78
12	8.69	2.02	6781.88	30.0	14.5	34.6	94.50	2.00	2.55	5.05	16	74
13	9.6	1.94	18287.72	19.5	14.4	34.6	93.23	1.83	3.30	4.90	17	87
14	6.75	2.03	14767.33	20.6	14.7	34.6	94.67	1.83	2.28	4.51	9	89
15	9.74	2.10	12019.51	23.3	14.4	34.7	93.61	1.76	2.74	4.48	15.08	82

656 Table 2

657

658

Abbreviation	Cyst-based taxonomy	Motile stage-based taxonomy	Autotrophic or Heterotrophic	Mean %
ACHO	<i>Ataxodinium choane</i>	<i>Gonyaulax</i> spp. ?	A	0.3
ISPH	<i>Impagidinium sphaericum</i>	<i>Gonyaulax</i> spp. ?	A	< 0.1
LMAC	<i>Lingulodinium machaerophorum</i>	<i>Lingulodinium polyedra</i>	A	45.3
OCEN	<i>Operculodinium centrocarpum</i>	<i>Protoceratium reticulatum</i>	A	2.5

OISR	<i>Operculodinium israelianum</i>	<i>Protoceratium</i> spp. ?	A	< 0.1
PDAL	Cyst of <i>Pentapharsodinium dalei</i>	<i>Pentapharsodinium dalei</i>	A	5.4
SBEL	<i>Spiniferites belerius</i>	Unknown	A	2.3
SBEN	<i>Spiniferites bentorii</i>	<i>Gonyaulax digitale</i> ?	A	11.5
SDEL	<i>Spiniferites delicatus</i>	<i>Gonyaulax</i> spp. ?	A	0.6
SMEM	<i>Spiniferites membranaceus</i>	<i>Gonyaulax</i> spp. (<i>membranacea</i> ?)	A	6.3
SMIR	<i>Spiniferites mirabilis</i>	<i>Gonyaulax spinifera</i> ?	A	1.1
SRAM	<i>Spiniferites ramosus</i>	<i>Gonyaulax</i> spp. ?	A	4.1
BSPP	<i>Brigantedinium</i> spp.	<i>Protopteridinium</i> spp. ?	H	11.8
ESPP	<i>Echinidinium</i> spp.	<i>Protopteridinium</i> spp. ?	H	1.7
GCAT	Cyst of <i>Gymnodinium catenatum</i>	<i>Gymnodinium catenatum</i>	H	0.1
GSPP	Cyst of <i>Gymnodinium</i> spp.	<i>Gymnodinium</i> spp.	H	< 0.1
LSAB	<i>Lejeunecysta sabrina</i>	<i>Protopteridinium leonis</i> ?	H	0.1
PAME	Cyst of <i>Protopteridinium</i>	<i>Protopteridinium americanum</i> <i>americanum</i>	H	0.1
PSPP	Cyst of <i>Protopteridinium</i> spp.	<i>Protopteridinium</i> spp.	H	< 0.1
SNEP	<i>Selenopemphix nephroides</i>	<i>Protopteridinium subinerme</i>	H	0.2
SQUA	<i>Selenopemphix quanta</i>	<i>Protopteridinium conicum</i>	H	4.2
STEL	<i>Stelladinium stellatum</i>	<i>Protopteridinium compressum</i>	H	0.6
TAPP	<i>Trinovantedinium applanatum</i>	<i>Protopteridinium pentagonum</i>	H	0.8
VCAL	<i>Votadinium calvum</i>	<i>Protopteridinium oblongum</i> ?	H	0.7
VSPI	<i>Votadinium spinosum</i>	<i>Protopteridinium claudicans</i>	H	< 0.1
XAND	<i>Xandarodinium xanthum</i>	<i>Protopteridinium divaricatum</i>	H	0.1

659 Table 3

Figure captions:

Figure 1: a) Location of the study area in NW France. b) Zoom on the S Brittany area identified in a): main bays and rivers are highlighted in the map, as well as the investigated Bay of Quiberon (BQ). The ‘Mor Bras’ is a bathymetric depression bordering the southern coast of Brittany. c) Distribution of the 15 sampling sites within the BQ. The yellow arrows represent the residual gyrotory tidal currents (Vanney, 1965; Lemoine, 1989; Tessier, 2006). Maps are performed using the SHOM bathymetric data (SHOM, 2015. ‘MNT Bathymétrie de façade Atlantique’ (Homonim Project). http://dx.doi.org/10.17183/MNT_ATL100m_HOMONIM_WGS84). LAT = “Lowest Astronomical Tides”, chart datum.

Figure 2: Distribution maps of various palynological and environmental parameters within the BQ. a) Clustering of sampling stations according to the relative abundances of dinocyst taxa (using PAST v.1.75b; Hammer et al., 2001); b) Colorization of sampling stations according to their membership group in the cluster; c) Dinocyst concentrations (number of specimens/cm³); d) Dinocyst diversity (Shannon diversity index); e) Heterotrophic dinocyst taxa percentages; f) Proportion of the ‘deep foraminiferal assemblage’ regarding the total benthic foraminifera taxa (as described in section 2.); g) Bottom water oxygen concentrations; h) Percentages of grain-size classes.

Figure 3: a) Diagram representing the percentages of the main dinocyst taxa (greater than 2% on at least one study site), as well as the number of taxa and the total dinocyst concentration, for each BQ study sample. Sampling sites are classified according to water depth. Sample n°3 (with only 13 individuals counted) is highlighted in grey. The station numbers (to the left of

the diagram) are highlighted with the colors identified in the cluster (Fig. 2). b) Averaged percentages of the dominant dinocyst taxa recorded in the fifteen BQ samples.

Figure 4: Correlation matrix of the different environmental, foraminiferal and dinocyst taxa presented in Tables 2 and 3. A color gradient from blue to red is used to represent the correlation coefficients (blue is used for negative values and red for positive ones; the higher the absolute value (i.e. when it tends to 1), the darker the color). Regarding the other half of the matrix, only p-values below 0.1 are highlighted in light ($0.1 < p\text{-value} < 0.01$) and dark ($p\text{-value} < 0.1$) green.

Figure 5: Conceptual model presenting the taphonomic preservation bias impacting dinocysts (especially heterotrophics and dinocyst concentrations) in the shallow Bay of Quiberon, on either side of the 6 m bathymetric threshold. The red arrows represent dinocyst fluxes to the sediments. H/A: ratio Heterotrophic to Autotrophic dinocysts. Due to homogenized hydrological parameters of the surface waters within the BQ, we consider that the H/A ratio and nutrient concentrations remain stable at the BQ scale. Gradients for particle size, oxygen concentration, and dinocyst preservation are highlighted under the figure with horizontal thicker or thinner lines on either side of the 6m isobath, and gradients for oxygen concentration, sea-surface temperature and water column mixing are highlighted to the right of the figure with vertical thicker or thinner lines according to the BQ water depth.

Figure 6: a) Location of modern samples and core tops used in the inshore-offshore transect at the southern Brittany-scale. Map performed using the SHOM bathymetric data (SHOM, 2015. '*MNT Bathymétrie de façade Atlantique*' (Homonim Project). http://dx.doi.org/10.17183/MNT_ATL100m_HOMONIM_WGS84) and depths are given according to the chart datum. b) Selected dinocyst taxa percentages: heterotrophics vs. autotrophics for the first line and percentages of the major taxa based on a main autotrophic sum (i.e. excluding heterotrophics). Sites are presented, from right to left, according to their

708 distance from continental influences: LE for ‘Loire estuary’, BQ for ‘Bay of Quiberon’, CBT
709 for ‘Core CBT-CS11’, VK for ‘Core VK03-58bis’ and MD for ‘Core MD95-2002’).

710 **Table 1:** Geographic coordinates of sampling sites. Sampling depths (‘depth’ in the
711 correlation matrix of variables) are provided according to the chart datum (‘lowest
712 astronomical tides’).

713 **Table 2:** Values of the environmental quantitative parameters used in the correlation matrix of
714 variables for each sampling station (cf. Fig. 4).

715 **Table 3:** List of dinocyst taxa (and their thecate name) identified in this study, abbreviations
716 and percentages recorded in the averaged fifteen BQ surface sediment samples.

717